Membrane pilot plant trials of CO_2 separation from flue gas

Colin A. Scholes, Abdul Qader, Geoff W. Stevens and Sandra E. Kentish*

Cooperative Research Centre for Greenhouse Gas Technologies (CO2CRC), Department of Chemical and Biomolecular Engineering, The University of Melbourne, VIC, 3010, Australia

Abstract

Industrial trials of membrane separation of CO_2 from flue gas generated by a lignite fired power station are reported. A hollow fiber Air Products PRISM and a spiral wound Dow Filmtec® NF3838/30FF membrane were separately trialed. The CO_2 permeance and selectivity through the PRISM membrane fell significantly in the initial hours of operation, reflecting competitive sorption effects and concentration polarisation. Alternatively, the wet flue gas enabled a facilitated transport mechanism to operate for the NF3838/30FF membrane and the CO_2 permeance and selectivity increased significantly compared to the dry membrane. Standard correlations were able to simulate the pressure drops through the modules.

Keywords: Membrane, carbon dioxide, flue gas, pilot plant, facilitated transport

*sandraek@unimelb.edu.au

Introduction

Post-combustion carbon capture is the selective separation of CO_2 from flue gas to reduce carbon emissions and limit anthropogenic climate change. Membrane gas separation has been shown to be viable for this separation process (1), and when combined with cryogenic separation is economically competitive with established solvent absorption technology (2-4). Ideally, the membrane should have both high CO_2 permeance and high CO_2/N_2 selectivity; Merkel *et al*. (2) suggests that a CO_2 permeance of 1000 GPU and CO_2/N_2 selectivity above 20 is needed. Polymeric membranes are of interest because they have been commercialized for natural gas sweetening (5). An alternative approach is facilitated transport membranes, which have shown the potential to achieve permeances and selectivities substantially higher than conventional polymeric membranes (6, 7). This is because the CO_2 reacts with either mobile or fixed carrier species and is carried across the membrane in a reacted state. In the majority of cases the facilitated mechanism requires the membrane to be saturated with water. However, while many high performing polymeric membranes and facilitated transport membranes have been developed in the laboratory, there have been few industrial pilot plant studies of these two types of membranes in post combustion capture. This is partially because fabrication of the membrane material into hollow fibers or spiral wound modules at the scale necessary for pilot-scale testing has not been undertaken, and partly the lack of membrane pilot plants available for post-combustion capture.

Another critical issue for membranes in post-combustion capture is the pressure loss through the module. The flue gas is available only at ambient pressure and most workers have shown that it is more effective to draw a vacuum on the permeate side than to compress this feed (8). However, in this scenario, any pressure drop across the module directly impacts the transmembrane pressure ratio and hence the separation that can be achieved.

Here we report on a membrane gas separation pilot plant for post-combustion CO_2 capture which is part of the Cooperative Research Centre for Greenhouse Gas Technologies (CO2CRC) H3 project, a post-combustion CO_2 capture trial on a Victorian brown coal fired power station (9, 10). In particular two membrane modules are separately studied. The first is an Air Products PRISM module filled with asymmetric glassy polymeric hollow fibres and originally designed for air separation. The second is a commercial thin-film composite polyamide membrane (Dow NF3838/30FF) in a spiral wound module designed for nanofiltration applications, but one that the authors have previously shown acts as a facilitated transport membrane under humid feed conditions (11). Importantly, both membranes are

currently manufactured as large scale modules and therefore can be readily transitioned to a future large-scale carbon capture process.

Theory

The flux (J_i) of a gas i through a non-porous polymeric membrane can be related to the membrane area (A), membrane thickness (l), gas fugacity difference across the membrane (Δf) and the permeability of the gas through the membrane (P_i) by (12):

$$J_i = \frac{P_i.A.\Delta f_i}{l} \quad (1)$$

For ideal gases, the fugacity difference can be replaced with the partial pressure difference across the membrane. If the membrane thickness is not accurately known, such is the case for the asymmetric and composite membranes studied here, then gas performance is often presented in terms of permeance, P' (cm^3 (STP) cm^{-2} s^{-1} $cmHg^{-1}$, or GPU (10^{-6} cm^3 (STP) cm^{-2} s^{-1} $cmHg^{-1}$)):

$$P' = \frac{P}{l} \quad (2)$$

The ideal selectivity (α) of one gas, A, compared to another gas, B, within a membrane is defined as the ratio of the permeabilities or permeances of the two gases:

$$\alpha_{A/B} = \frac{P_A}{P_B} \quad (3)$$

The pressure drop for an ideal gas through the membrane module can be approximated, by assuming isothermal flow, as (13):

$$p_1^2 - p_2^2 = G^2 \frac{RT}{M}\left[\frac{4fL}{d_H} + 2\ln\left(\frac{p_1}{p_2}\right)\right] \quad (4)$$

where p_1 and p_2 are the inlet and exit pressures respectively (Pa), G is the mass velocity ($kg/m^2.s$), R is the universal gas constant (8.314 J/mol.K), M is the molecular weight ($kg.mol^{-1}$), f is the Fanning friction factor, L is the module length (m) and d_H the hydraulic mean diameter (m).

For spiral wound modules, the flow behavior and corresponding pressure drop is critically dependent on the presence of the spacer material between the membrane sheets (14, 15). The spacer material

reduces the void volume and hence effectively increases the chaotic flow. As a result, the spacer type and orientation impacts the hydraulic diameter of the flow channel (16, 17):

$$d_h = \frac{4\varepsilon}{\frac{2(b+h)}{bh}+(1-\varepsilon)S_{V,SP}} \quad (5)$$

where ε is porosity of the spacer, b the width of the membrane, h the channel height or spacer thickness and $S_{V,SP}$ is the specific surface of the spacer.

For laminar flow through the lumen side of the hollow fibre module, the friction factor can be determined from the well known expression for pipe flow:

$$f = \frac{16}{Re} \quad (6)$$

Experimental

The membranes studied were an Air Products PRISM PA1020 membrane and a Dow Filmtec® NF3838/30FF membrane. The PRISM membrane is an asymmetric hollow fiber polysulfone membrane, while the NF3838/30FF membrane has a surface layer that is a polypiperazine amide with the presence of free amine and carboxylate end groups; coated on a polysulfone interlayer over a polyester support. The PRISM membrane was housed in a polycarbonate module, while the NF3838/30FF membrane was housed within a fiber-glass module (Alfa Laval). Details on both membranes can be found in Table 1. For the PRISM membrane, the area and number of fibers was estimated based on the internal cross-sectional area of the module. Both membranes were mounted horizontally in the pilot plant (Figure 1) but trialed separately.

The pilot plant studies were undertaken on a custom built plant as part of the CO2CRC H3 Capture project (9), using flue gas from a Victorian brown coal fired power station. The flue gas was taken after the blower discharge of a direct contact cooler. The average feed gas composition is provided in Table 2; though composition varied considerably between days, dependent on the operation of the power station. The flue gas pressure was increased further to ~150 kPaa by a feed booster and subsequently cooled through a plate heat exchanger to ambient conditions. A separator vessel removed any condensed water and the flue gas was then reheated to ~ 45 ^{o}C through trace heating. The dew point of the flue gas varies between 5 and 20 ^{o}C. To control the feed pressure, a control valve on the feed line

was used to divert a proportion to a bypass line. The feed flowrate (1 to 3.5 kg/hr) was measured through a flow indicator (Aalborg), while the retentate flowrate was controlled through a flow controller (Aalborg). For the hollow fibre module, the feed gas was on the lumen side. The permeate stream was under vacuum (liquid ring pump), with the permeate discharge into a separator vessel for removal of water. Pressures were measured on the feed, retentate and permeate lines. The permeate pressure for both membranes was ~11 kPaa, with a pressure ratio of feed to permeate ~12. For the PRISM membrane the stage cut was between 0.18 and 0.25, while for NF3838/30FF membrane the stage-cut was 0.16 to 0.28, dependent on Reynolds number. All lines were discharged into the blower suction of the main capture plant onsite, with one-way valves ensuring no back flow. The PRISM membrane was operated for a total of 24 hours and the NF3838/30FF membrane was operated for a total of 98 hours.

The presence of condensed water throughout the membrane pilot plant was a constant challenge. This was because of the fluctuating humidity of the feed flue gas; and fluctuating gas temperatures in the un-insulated small bore feed supply piping with ambient temperature fluctuations. Such water condensation is often avoided in other membrane gas separation processes, such as natural gas processing, by having an extensive dehydration process upstream (18).

All gas samples were analyzed through an onsite CO_2 analyzer (Servomex), and also measured by gas chromatography (Varian CP-3800, column Molecular Sieve and PORAPAK Q in series).

Figure 1

Table 1

Table 2

Results and Discussion

PRISM Membrane

The CO_2 permeance (GPU) as a function of time for the Air Products PRISM membrane is provided in Figure 2. The initial permeance is 763 GPU, which is near the suggested minimum for competitive membrane processes (2). However, the initial ideal selectivity is only $CO_2/N_2 = 13$ (Figure 3), which is almost half that reported in the literature for similar membranes under pure gas conditions (19, 20). The value is also substantially lower than that recorded for dry mixtures of 10% CO_2 in N_2, where the selectivity has been observed to increase to values as high as 40 (20). However, the initial N_2 permeance of 57.9 GPU is comparable to that estimated from air separation performance, 64.2 GPU (21). The lower selectivity probably reflects competitive sorption from other flue gas components in the membrane, including water, SOx and NOx, as well as the impacts of CO_2 plasticisation, which will also reduce selectivity. A similar loss of selectivity under mixed gas conditions has been observed in other glassy polymeric membranes (20, 22-24).

The CO_2 permeance and selectivity both decrease rapidly over the first 5 hours of operation to 265 GPU and $CO_2/N_2 = 4$. This loss of permeability and selectivity may be related to further competitive sorption from increasing concentrations of water. For example, a similar reduction in CO_2 permeability is recorded in a fluorinated polyimide (6FDA-TMPA) when the water activity is increased from zero to 0.8 (22). Conversely, while Paulson et al. (24) observed a significant decrease in selectivity, these authors observe a flux increase for a CO_2/CH_4 methane mixture through a polysulfone membrane when the gas stream was humidified. However, their water concentrations (1 mol%) are significantly lower than those observed here (~ 10 mol%).

Secondly, the decrease in CO_2 permeance and selectivity may be attributed to the onset of concentration polarisation, given that the N_2 permeance increases with time. That is, there will be a build up of the less permeable gas species on the membrane surface due to mass transfer limitations within the boundary layer of the fluid flow. This build up will reduce the partial pressure of carbon dioxide and increase that of nitrogen, resulting in an observed loss of both permeance and selectivity. It is common in membrane processes such as ultrafiltration to observe a rapid decline in permeance for the same reason. Finally, while there was very limited visual evidence of membrane fouling, it is possible that deposits of fly ash on the internal surface of the membrane fibres limited the flow of gas directly,

and also enhanced the concentration polarisation, by limiting the mass transfer coefficient at the membrane surface (25).

After this 5 hour period the CO_2 permeance and selectivity both recover slowly, obtaining an average value of 480 GPU and CO_2/N_2 = 5 after ~ 15 hours. The gradual increase in permeance may be associated with the sorbed water swelling or plasticizing the membrane, which increases the fractional free volume and hence the CO_2 diffusivity through the membrane. Again, similar behavior has been observed in the literature (26, 27). The membrane module never regained its initial performance, even under dry conditions, and the exposure to the wet flue gas had a permanent impact on the membrane. Importantly this result indicates that the CO_2 permeance of the PRISM membrane achieves an average value that is 61 % of the initial performance. Hence, under saturated conditions the CO_2 permeance of the PRISM membrane is half that suggested for membrane gas separation to be economically competitive. Similarly the observed CO_2/N_2 ideal selectivity is too low and makes this membrane unsuitable for post-combustion capture.

Figure 2

Figure 3

The low concentration of the minor components in the flue gas, specifically CO, NOx and SOx, has meant quantitative determination of the permeances through the membrane was not possible. Qualitative measurements were undertaken to determine the percentage of each minor component that is transferred to the permeate stream, and are provided in Table 3. It is clear that only a small amount of CO transfers through the membrane to the permeate stream, and therefore CO permeance is lower than CO_2, as supported by the literature (20). In contrast, the majority of NOx and SOx in the feed gas are transferred to the permeate stream. This indicates that both minor component gas classes have high permeance and will enrich the permeate stream. This is expected because of the strong condensability of these gases, especially NO_2 and SO_2, which for glassy polymeric membranes strongly correlates with gas permeability (23). There was only minor evidence of ash build-up in the membrane fibers and module, and no visual degradation of the hollow fibers was observed at the end of the trial period.

Table 3

NF3838/30FF Membrane

The near saturated flue gas conditions are beneficial for the NF3838/30FF membrane because of a facilitated transport mechanism that arises due to the presence of piperazine functional groups and free amine within the membrane structure (11). The dry and wet pure gas permeance and selectivity for the NF3838/30FF membrane are summarised in Table 4, from our previous work (11). As noted in this work, the CO_2 permeance in the laboratory varied from 8 to 340 GPU, dependent upon the degree of water saturation, the feed gas composition and the feed gas pressure. However, in general the performance under wet gas conditions substantially exceeds that under dry conditions, due to this facilitated transport mechanism.

Table 4

The CO_2 permeance of this membrane in the pilot plant with time is provided in Figure 4 and the CO_2/N_2 selectivity in Figure 5. The CO_2 permeance and selectivity are both initially low, but contrary to the results with the PRISM membrane, they increase over a 20 hour period. This reflects the membrane becoming wet and the facilitated transport mechanism coming into play. After 20 hours of operation the CO_2 permeance has reached a steady-state of ~29 GPU and the CO_2/N_2 selectivity is around 7. The N_2 permeance remains relatively constant over this time period. This is a similar selectivity to that observed in the laboratory for a similar mixture of 10 % CO_2 in N_2 under humid conditions [9], but around half the permeance. The lower permeance may reflect the facilitated transport carriers being utilised by other acid gas components such as SO_2 and NO_2; the effects of concentration polarisation or fouling; or that parts of the membrane were not being completely saturated. At the 48 hour mark (Point A) the membrane module was not operated for a 1 week because of extreme temperatures onsite, > 40 ^{o}C. This resulted in the membrane drying out and CO_2 permeance performance returning to dry conditions when trials continued. Exposure to the wet flue gas resulted in an increase in both the permeance and selectivity again to values equal to that observed before the week long shut down. This demonstrates that a near saturated flue gas feed is constantly required to maintain the facilitated transport mechanism. Overall, it is clear the membrane is able to achieve a facilitated transport mechanism

supported by the saturated flue gas, however neither the CO_2 permeance or CO_2/N_2 ideal selectivity are of the order necessary to enable this membrane to be competitive for post-combustion capture.

Figure 4

Figure 5

There was no evidence of carbon monoxide in the permeate stream, implying that it does not pass through the NF3838/30FF membrane. NOx and SOx were also not detected in the permeate stream. This latter result is somewhat surprising and may reflect an irreversible reaction of these strongly acid gases with the piperazine and amine functional groups within the membrane. However, there was no evidence of membrane degradation due to such interactions. There was evidence of ash build-up at the feed entry to the spiral wound module, but no evidence of ash accumulation within the membrane spacer.

Module Pressure Drop

It is difficult to compare the pressure drop through the hollow fibre module to literature values as the number of fibres and the fibre dimensions are not accurately known. In the present case, we measured the outer diameter of the fibres using optical microscopy to be 0.25 mm. We then estimated the number of fibres based upon these being arranged within a close hexagonal packing arrangement within the 35 mm diameter module, giving around 11,000 fibres. Simulation of the pressure drop through the module, based upon Equations 4 and 6, then gave a good fit to the data with a fibre internal diameter of 0.16 mm, suggesting a wall thickness of 45 micron (Figure 6). These data are consistent with literature examples of commercial hollow fibres. This analysis also allowed the Reynolds numbers for this data to be estimated.

The relevant dimensions could be determined for the spiral wound module, using a combination of supplier's data, our own measurements and estimates from the literature. However, in this case, the

Fanning friction factor was unknown, as the flow pattern inside the module was not necessarily laminar. In this case, simulation using Equations 4 and 5 was used to estimate this friction factor. The resulting values are in the range of 0.2 to 0.4 for a Reynolds Number range of 4 to 15. This is consistent in magnitude with those quoted by Shakaib *et al*. (0.15-0.3) (28) and Geraldes *et al*. (0.1 to 1.0 in the Reynolds number range of 100 to 10) (29)We believe that this is the first time that such an analysis of pressure drop has been completed for gas flow through a spiral wound module and it is noteworthy that Equation 5, developed for liquid phase operations such as reverse osmosis and ultrafiltration appears to still hold in this situation. These correlations are independent of the mechanism for CO_2 transport through the membrane; both for solution diffusion in the case of the PRISM membrane and facilitated transport in the case of the NF3838/30FF membrane.

The pressure drop from the feed to retentate across both membrane modules is provided in Figure 7 as a function of feed gas Reynolds Number in the respective module. The pressure drop through the hollow fiber module is nearly two orders of magnitude greater than the pressure drop across the spiral wound module, even at comparable Reynolds numbers. This difference is due to the respective geometry of the membrane modules, with the feed gas passing through very small bore hollow fibers relative to the wider spacer between membrane sheets in the spiral wound module. Wider bore hollow fibers will reduce the pressure loss experienced, with a hollow fiber of internal diameter ~5.3 mm estimated to provide the same pressure drop across the module length as that observed for the spiral wound module. Alternatively, a much greater number of fibres could be used. However, in practice, it would also be better to pass the feed gas through the shell side of the module, as shell side flow may ultimately cause fewer issues with any buildup of ash fouling.

Figure 6

Figure 7

Energy Duty and Economic Viability

The electrical energy consumption of the membrane pilot plant, inclusive of the blower and vacuum pump was ~5 MJ/kg of CO_2 captured, dependent upon the feed flowrate and the membrane module used. Given that around three times this quantity of thermal energy would be needed to generate the

necessary electrical energy, this is considerably higher than energy duties reported in the literature for for amine based solvent capture (3.7 to 5.9 MJ/kg(30). However, it should be stressed that the purpose of the membrane pilot plant was to test the performance of membranes and membrane modules for CO_2 capture in the field and minimising the energy duty was not the focus. Detailed simulation studies of membrane gas separation processes for CO_2 capture from flue gas have indicated that the electrical energy duty can approach 1 MJ/kg of CO_2 captured (2, 3, 31), dependent on the flue gas composition and membrane process design. The same literature studies have indicated that the cost of capture for membrane technology can approach US$ 32 per tonne of CO_2 avoided for a fully integrated process design.

Conclusion

A hollow fiber PRISM membrane and a spiral wound NF3838/30FF membrane were trialed on an industrial pilot plant for the separation of CO_2 from flue gas. The fluctuating water load through this system was the most challenging operational issue encountered during the trials. The CO_2 permeance and CO_2/N_2 selectivity of the hollow fibre module decreased considerably upon exposure to the flue gas, reflecting competitive sorption from the water, concentration polarisation and possibly membrane fouling. The sorption of water into the PRISM membrane resulted in reduced separation performance and this membrane was not suited for post-combustion capture of CO_2. Conversely, the CO_2 permeance of the spiral wound membrane increased in the presence of flue gas, because the saturated water conditions allowed a facilitated transport mechanism to operate. This also increased the CO_2/N_2 selectivity of the NF3838/30FF membrane. However, both CO_2 permeance and CO_2/N_2 selectivity did not achieve the same level observed in the laboratory, again possibly due to competition from other acid gases, concentration polarisation or fouling. In addition, the lower performance in this case could also imply that regions of the membrane were not fully saturated.

Pressure drop correlations from the literature were able to accurately model the observed pressure behaviour, confirming that these correlations, while developed for liquid phase filtration, could be applied to gas separation processes. These pressure drop calculations suggested that spiral wound module configurations comparable to those used in nanofiltration will be suitable for post combustion capture. Conversely, hollow fibre modules such as those used in current gas separation applications may not provide sufficient cross sectional flow areas and larger bore systems may be required.

Acknowledgements

The authors would like to thank GDF SUEZ Australian Energy, Hazelwood for facilitating the installation and operation of the pilot plant in their premises and for access to equipment, as well as the contributions of Sang Yun Andrew Lee and Alita Aguiar. Funding for this CO2CRC project is provided by the Australian Government through its Cooperative Research Centre program as well as the Particulate Fluids Processing Centre of the University of Melbourne.

References

1. Koros WJ. Gas Separation. In: Baker RW, editor. Membrane Separation Systems. Park Ridge: William Andrew Publishing; 1991.
2. Merkel TC, Lin H, Wei X, Baker R. Power plant post-combustion carbon dioxide capture: an opportunity for membranes. J Membrane Sci. 2010;359:126-39.
3. Scholes CA, Ho MT, Wiley DE, Stevens GW, Kentish SE. Cost competitive membrane - cryogenic post-combustion carbon capture. Int J Greenhouse Gas Control. 2013;17:341-8.
4. Hasse D, Kulbarni S, Sanders E, Corson E, Tranier JP. CO2 capture by sub-ambient membrane operation. Energy Procedia. 2013;37:993-1003.
5. Scholes CA, Stevens GW, Kentish SE. Membrane gas separation applications in natural gas processing. Fuel. 2012;96:15-28.
6. Ward WJI, Robb WL. Carbon dioxide-oxygen separation: facilitated transport of carbon dioxide across a liquid film. Science. 1967;156:1481-4.
7. Nakabayashi M, Okabe K, Fujisawa E, Hirayama Y, Kazama S, Matsumiya N, et al. Carbon dioxide separation through water-swollen-gel membrane. Energy Convers Mgmt. 1995;36:419-22.
8. Ho MT, Allinson GW, Wiley DE. Reducing the cost of CO2 capture from flue gases using membrane technology. Ind Eng Chem Res. 2008;47:1562-8.
9. Qader A. Demonstrating carbon capture. The Chemical Engineer. 2009;November:52-3.
10. Scholes CA, Qader A, Stevens GW, Kentish SE. Membrane gas-solvent contactor pilot plant trials of CO2 absorption from flue gas. Sep Sci Technol. 2014;49:2449-58.
11. Lee SA, Stevens GW, Kentish SE. Facilitated transport behavior of humidified gases through thin-film composite polyamide membranes for carbon dioxide capture. J Membrane Sci. 2013;429:349-54.
12. Yampol'skii YP. Polymeric gas separation membranes. Boca Raton, FL: CRC Press; 1994.
13. Tilton JT. Fluid and Particle Dynamics. In: Green DW, Perry RH, editors. Perry's Chemical Engineers' Handbook, . 7th Edition ed. Singapore: McGraw-Hill; 1998.
14. Da Costa AR, Fane AG, Wiley DE. Spacer characterization and pressure drop modelling in spacer-filled channels for ultrafiltration. J Membrane Sci. 1994;87:79-98.
15. Schwinge J, Neal PR, Wiley DE, Fletcher DF, Fane AG. Spiral wound modules and spacers. Review and analysis. J Membrane Sci. 2004;242:129-53.
16. Schwinge J, Wiley DE, Fletcher DF. Simulation of the flow around spacer filaments between narrow channel walls. 1. Hydrodynamics. Ind Eng Chem Res. 2002;41:2977-87.

17. Schock G, Miquel A. Mass transfer and pressure loss in spiral wound modules. Desalination. 1987;64:339-52.
18. Baker R. Vapor and gas separation by membranes. In: Li NN, Fane AG, Ho WSW, Matsuura T, editors. Advanced membrane technology and applications. Hoboken, New Jersey: John Wiley & Sons; 2008.
19. McHattie JS, Koros WJ, Paul DR. Gas transport properties of polysulfone. 2. Effect of bisphenol connector groups. Polymer. 1991;32:2618-25.
20. Scholes CA, Chen GQ, Stevens GW, Kentish SE. Nitric oxide and carbon monoxide permeation through glassy polymeric membranes for carbon dioxide separation. Chem Eng Res Des. 2011;89:1730-6.
21. PRISM PA1020 Nitrogen membrane separation module. Air Products, 2007.
22. Chen GQ, Scholes CA, Doherty CM, Hill AJ, Qiao GG, Kentish SE. Modeling of the sorption and transport properties of water vapor in polyimide membranes. J Membrane Sci. 2012;409-410:96-104.
23. Scholes CA, Kentish SE, Stevens GW. Effects of minor components in carbon dioxide capture using polymeric gas separation membranes. Sep Purif Reviews. 2009;38:1-44.
24. Paulson GT, Clinch AB, McCandless FP. The effects of water vapor on the separation of methane and carbon dioxide by gas permeation through polymeric membranes. Journal of Membrane Science. 1983;14(2):129-37.
25. Hoek EMV, Elimelech M. Cake-Enhanced Concentration Polarization: A New Fouling Mechanism for Salt-Rejecting Membranes. Environmental Science & Technology. 2003;37(24):5581-8.
26. Watari T, Wang H, Kuwahara K, Tanaka K, Kita H, Okamoto KI. Water vapor sorption and diffusion properties of sulfonated polyimide membranes. J Membrane Sci. 2003;219:137-47.
27. Potreck J, Nijmeijer K, Kosinski T, Wessling M. Mixed water vapor/gas transport through the rubbery polymer PEBAX 1074. J Membrane Sci. 2009;338:11-6.
28. Shakaib M, Hasani SMF, Mahmood M. CFD modeling for flow and mass transfer in spacer-obstructed membrane feed channels. Journal of Membrane Science. 2009;326(2):270-84.
29. Geraldes Vt, Semião V, de Pinho MN. Flow management in nanofiltration spiral wound modules with ladder-type spacers. Journal of Membrane Science. 2002;203(1–2):87-102.
30. Desideri U, Paolucci A. Performance modelling of a carbon dioxide removal system for power plants. Energy Conversion and Management. 1999;40(18):1899-915.
31. Scholes CA, Ho MT, Aguiar AA, Wiley DE, Stevens GW, Kentish SE. Membrane gas separation processes for CO2 capture from cement kiln flue gas. Int J Greenhouse Gas Control. 2014;24:78-86.

Table Captions

Table 1: Membrane module characteristics based on a combination of suppliers' information, direct measurement and comparable literature values.

Table 2: Average composition of the flue gas (vol % dry basis).

Table 3: The percentage of minor components in the feed gas that transferred to the permeate stream.

Table 4: Permeation (GPU) of dry and humidified pure gases at 35 ^{o}C and 400 kPa, taken from Lee *et al*. (11).

Figure Captions

Figure 1: Membrane module on site at the membrane pilot plant, as part of the CO2CRC H3 project.

Figure 2: CO_2 Permeance (GPU) of PRISM membrane over time (hours).

Figure 3: CO_2/N_2 Selectivity of PRISM membrane over time (hours).

Figure 4: CO_2 permeance (GPU) through NF membrane as a function of time exposed to flue gas.

Figure 5: CO_2/N_2 selectivity through NF membrane as a function of time exposed to flue gas.

Figure 6: The variation in the squared pressure difference across the hollow fibre module as a function of the Reynolds number, both as observed experimentally and as calculated from Equations 4 and 7, assuming an internal fibre diameter of 0.16 mm and 11,000 fibres.

Figure 7: Pressure drop (kPa) of the flue gas through the PRISM hollow fiber and NF3838/30FF spiral wound membrane modules as a function of Reynolds No.

Tables

Table 1

	PRISM Membrane	NF3838/30FF
	Hollow fiber	Spiral wound
Area (m^2)	~ 5[3]	7.5[1]
Length (m)	0.55[2]	0.965[2]
Module internal diameter (m)	0.035[2]	0.099[2]
Fiber OD (mm)	0.25[2]	-
Fiber ID (mm)	0.16[5]	-
No. of Fibers	~11,000[3]	-
Hydraulic Mean Diameter(mm)		0.33[4]

[1] Specified by the manufacturer; [2] measured experimentally; [3]calculated through geometrical calculations; [4]assumed based on comparable values in the literature; [5]calculated from pressure drop

Table 2

	Composition (vol % dry)
CO_2	12
N_2	80.5
O_2	7.5
CO	246 ppm
SOx	96 ppm
NOx	108 ppm
Water	0.2 m^3/m^3 flue gas

Table 3

	% of Feed stream that transfers to the permeate
CO	13.1 ± 2.0
NOx	82.4 ± 16.4
SOx	87.4 ± 11.8

Table 4

	Dow NF3838/30FF		
	$P(N_2)$ (GPU)	$P(CO_2)$ (GPU)	CO_2/N_2
Dry (pure gas)	3.7	10	2.8
Wet (pure gas)	1.8	34-340*	19-50*
Dry (10 % CO_2 in N_2)	6.5	8	1.3
Wet (10 % CO_2 in N_2)	7	55	7

*Dependent upon water saturation, water pH and feed gas pressure

Figures

Figure 1

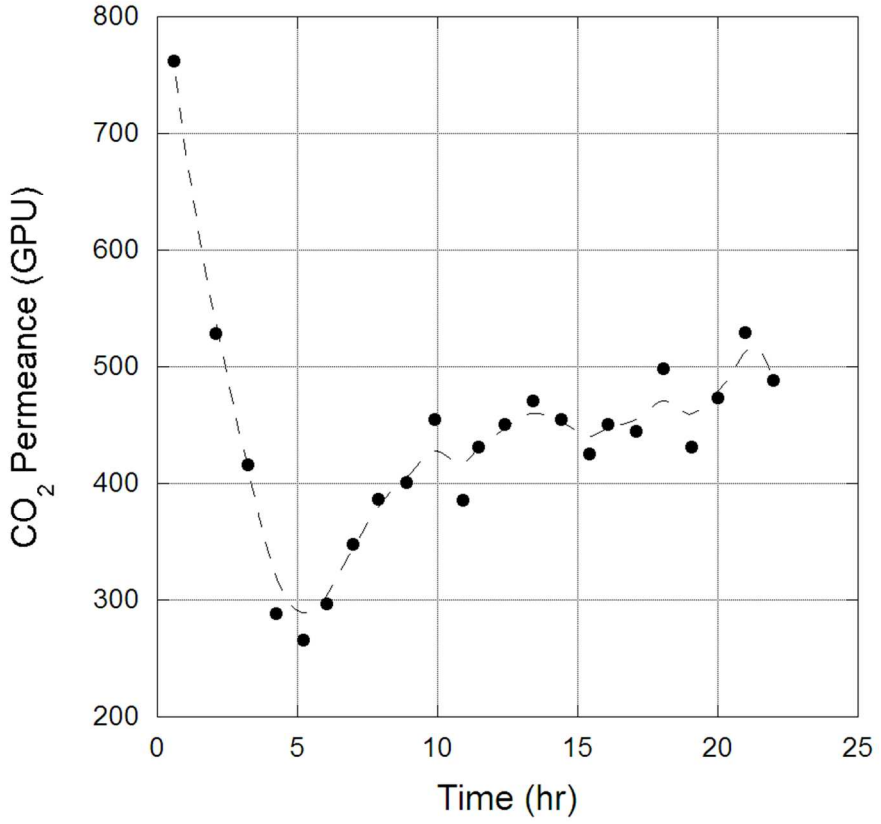

Figure 2

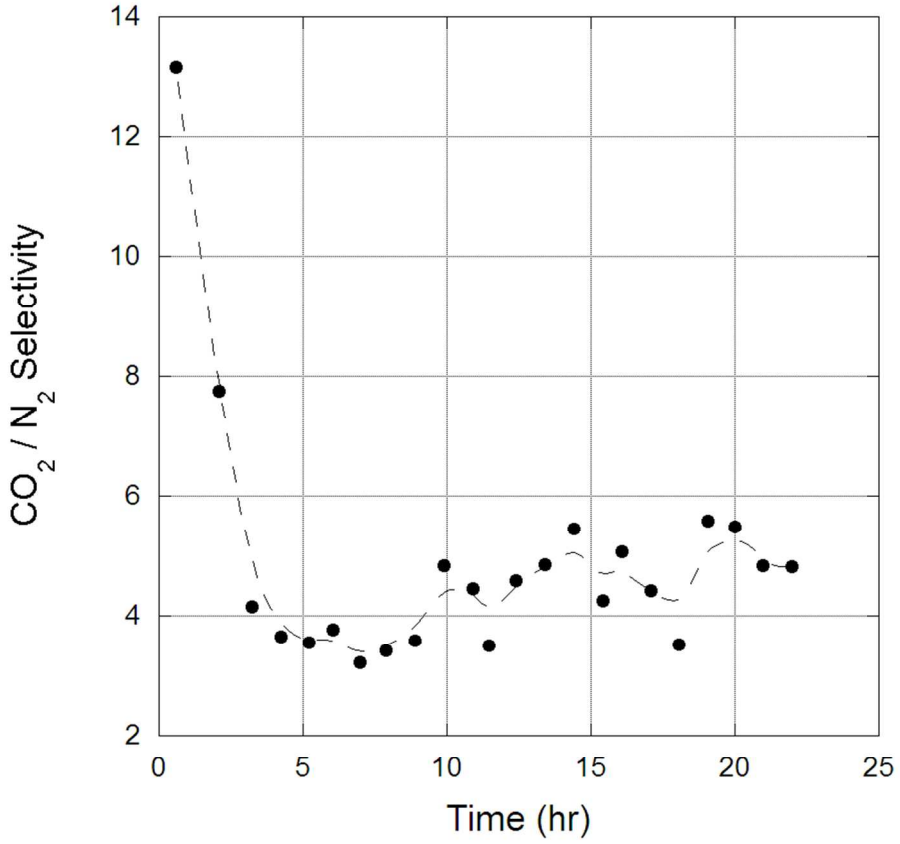

Figure 3

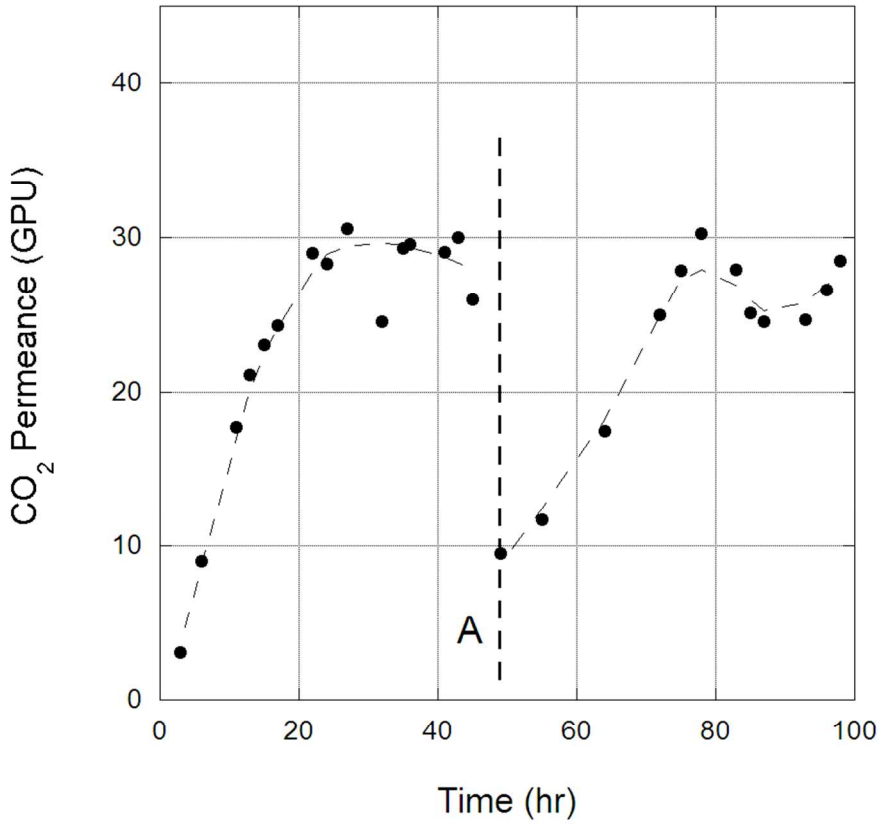

Figure 4

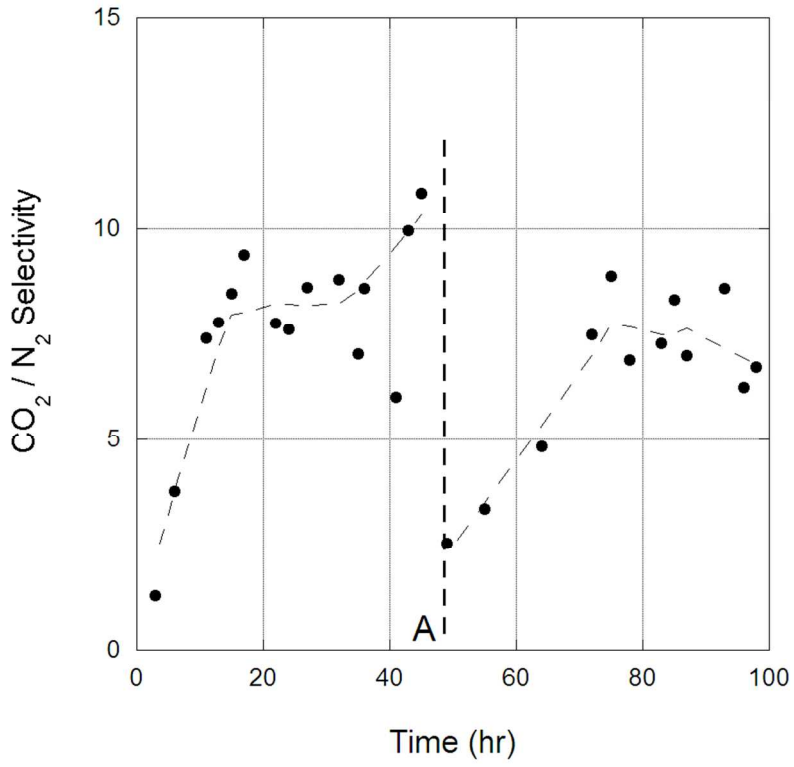

Figure 5

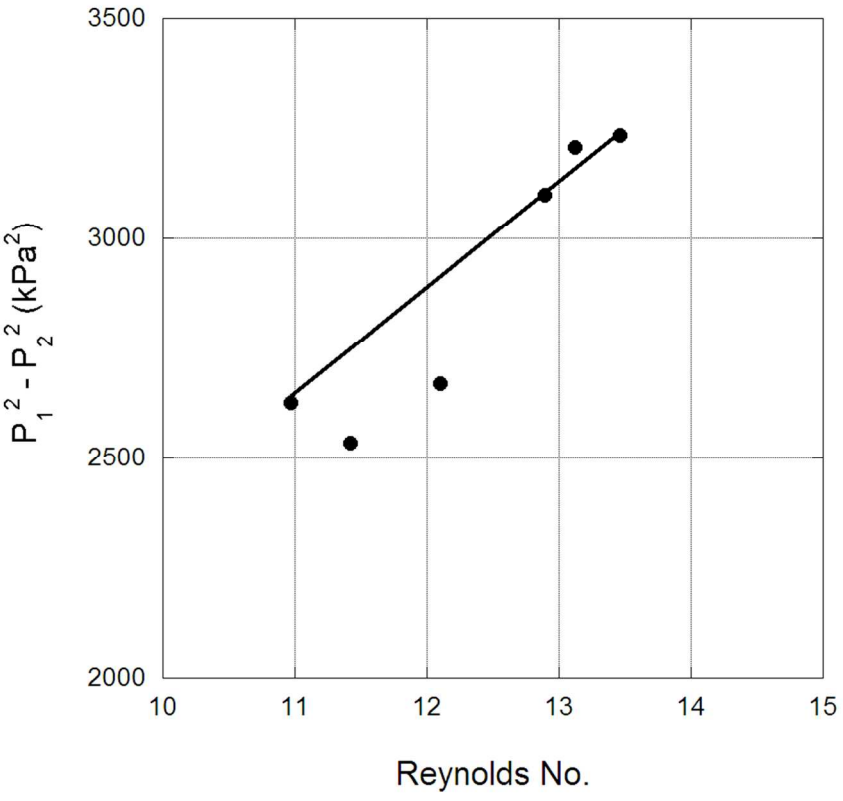

Figure 6

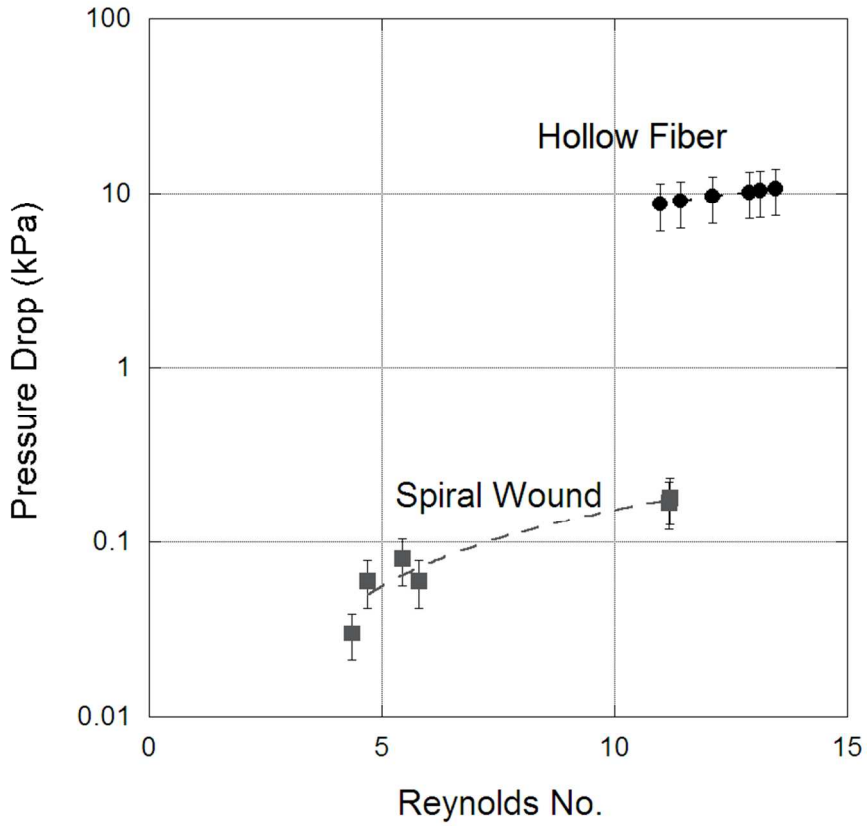

Figure 7